

Supplementary Information: Torque-Dense Photomechanical Actuation

Stiffness Comparison in Flat and Curved Structures

Bending stiffness of a flat and a curved structure (made of rectangular 10mm(W) × 6mm(L) × 50 μm ALCP sheet) are qualitatively compared by attaching weight of a 2 gr to the tip of both structures. At this specific loading condition, the flat structure bends while no bending is observed in the curved structure.

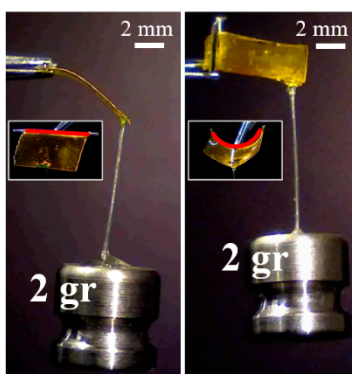


Figure SI1: Comparison of the bending stiffness for flat and curved samples of same size. Flat sample (left) bends while the curved sample (right) stays undeformed. The inset shows the cross section of samples with the red line highlighting the flat and curved geometry.

Characterization of Splayed ALCP

After synthesizing ALCP (50 μm), a 5mm × 5mm squared sheet was cut from the sample and was characterized using polarized optical microscopy.

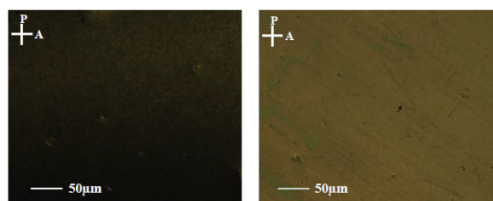


Figure SI2: Polarized optical microscopy (POM) images of splayed ALCP under cross polarizers which the planar alignment is 0° and 45° corresponding to the polarizer.

Behavior of a flat ALCP actuator

Sample with a flat cross-section was fabricated by attaching a wire along its periphery but keeping it straight. A load was attached to the tip of the actuator and irradiated. The actuation is quasistatic, in comparison to that observed in SI Movie 5, when a transverse curvature is imposed.

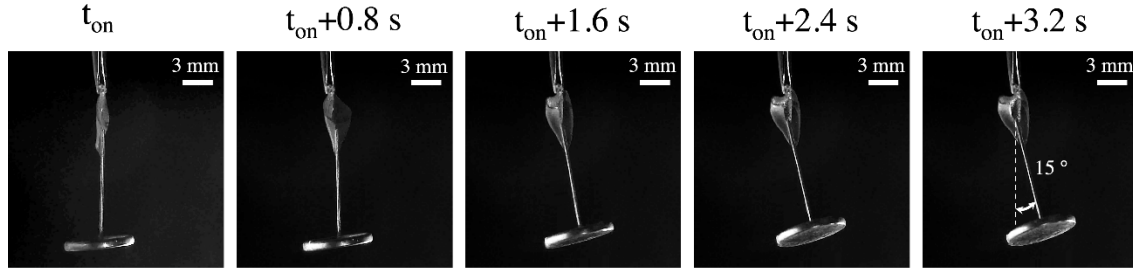


Figure SI3: Time sequenced images of the progressive quasistatic actuation of a loaded actuator, when the Cu wire is straight and the ALCP is flat.

Fabrication of the Boundary Constrained ALCP Actuators

A rectangular shape splayed ALCP (10mm×6mm) was cut from a thin film of 50 μm thickness (Figure SI4.a-b). Using a commercially available acrylate-based glue, a copper wire was glued along the longer edge of the sample (10 mm) and on the surface with planar nematic direction (Figure SI4.c). The ALCP film and the wire were wrapped around a cylinder with the desired diameter in a way that the planar surface and the wire were on the convex side (Figure SI4.d). The two free ends of the wire are connected to fix the curvature and is later used to hold the sample in front of the UV source with a tweezer (Figure SI4.e)

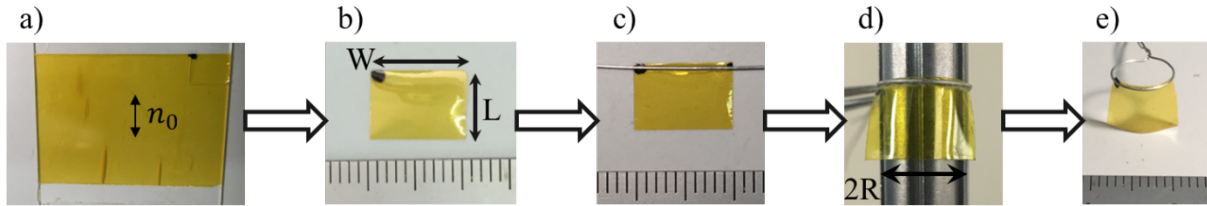


Figure SI4: Fabrication of boundary confined shell using ALCP films. The scale is in mm.

Torque Calculation

The torque (τ), angular momentum (L), and energy (KE) are related by:

$$\tau = \dot{L} = \frac{dL}{dt} = \frac{dI\omega}{dt} = I \frac{d\omega}{dt} = I\alpha$$

$L = I\omega$ with I , the moment of inertia and ω , the angular velocity. Kinetic energy (KE) is:

$$KE = \frac{1}{2}I\omega^2 = \frac{1}{2}L\omega$$

From the balance of internal power, in the absence of external forces:

$$\int P_{int} dv + \frac{D}{Dt} KE = \int P_{out} dv, P_{out} = 0$$

$$\frac{D}{Dt} KE = \frac{D}{Dt} \left(\frac{1}{2} L \omega \right) = \left(\frac{1}{2} \dot{L} \omega + L \dot{\omega} \right) = \left(\frac{1}{2} \tau \omega + L \alpha \right) = \tau \omega$$

where P indicates the stress power (rate of change of strain energy density). For the Neo-Hookean material, with $\dot{W} = P_{int}$, we find that:

$$\int \dot{W} dv + \tau \dot{\phi} = 0$$

And,

$$\tau \Delta \phi = \tau \dot{\phi} = -\Delta \psi$$

This equation is used for determining the torque density generated in the system. Using the equation above and conducting COMSOL simulations for various geometrical parameters we can get the trends shown in Figure SI3 for torque density of prebiased actuators and the photostrain that is required to get the snap-through.

Torque-Density as a Function of Geometry of the Photoactuators.

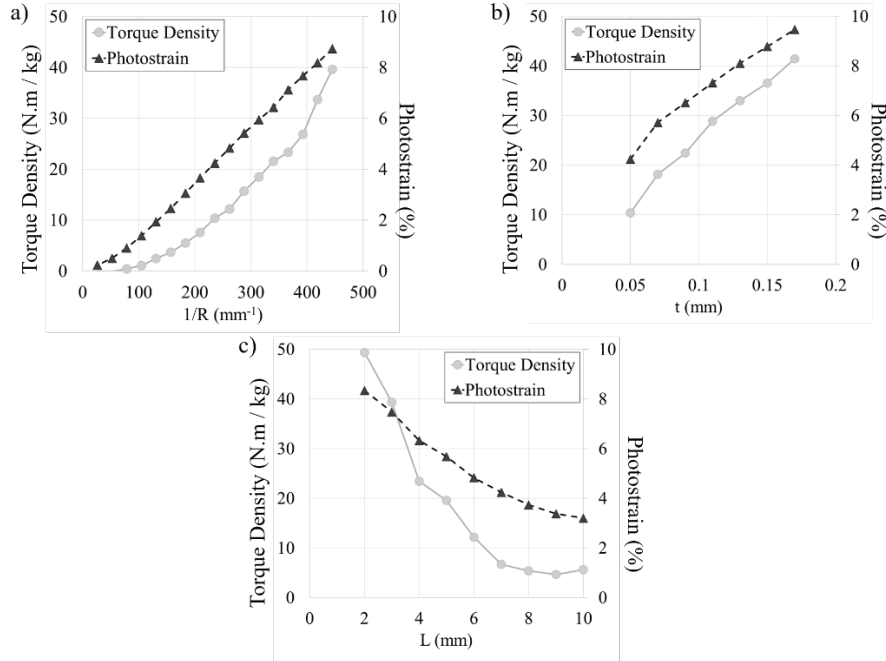


Figure SI5: Torque density as a function of initial curvature, thickness of the film and length of the film. The photostrain values correspond to that needed to trigger the instability. Torque density is measured as a function of a) the radius (R) of the transversely curved shell. b) thickness (t) of the actuator and c) the length of the actuator

In these simulations all geometrical parameters except one are kept constant. As can be seen in Figure SI5.a, by increasing the initial curvature of the actuator (smaller R) we get higher generated torque densities. This comes at a price. Higher torque densities require larger photostrain that is

generated along the nematic director. The tradeoff is repeated as a function of thickness (t) in Figure SI5.b. The effect of actuator's length (L) in the rotary actuation is presented in Figure SI5.c. The results obtained from these simulations show the longer actuators make for weaker rotary actuators.

Geometric Scaling of Curved Crease Photoactuators

A parameter that play a significant role in determining the development of the instabilities is ϕ , the bending angle at the hinge immediately after the snap-through. Assuming a constant first principal curvature that is defined by the prebiased curvature, $\kappa_1 = \kappa_0 = 1/R$, the second principal curvature at the location of the curved crease can be determined using the angle ϕ , where:

$$\kappa_2 = \frac{1}{R_c} = \frac{\phi}{w_c}$$

We assume that the snap-through leads to an isometric transformation from the transversely curved shell to a segmented geometry. Here, translation arises along the sample's length and involves a mirror symmetry about the osculating plane. The osculating plane forms the bisector of ϕ (1). The folding curve that defines the hinging during the creasing is composed of the ends near the edges of the sample, where they are affixed and the vertex of the crease (Figure 3b). Thus, ϕ can be written as,

$$\phi = 2 \arctan \left(\frac{R \left(1 - \cos \left(\frac{\theta}{2} \right) \right)}{l} \right) \sim \frac{R\theta^2}{l}$$

where R and θ are as defined in Figure 3b. l is from the fixed boundary, and essentially, $l = L$. Thus, the angle of actuation scales with $\frac{R\theta^2}{L} = W^2/RL$, as shown in the in Figure 3d.

Repetitive Actuation Cycles

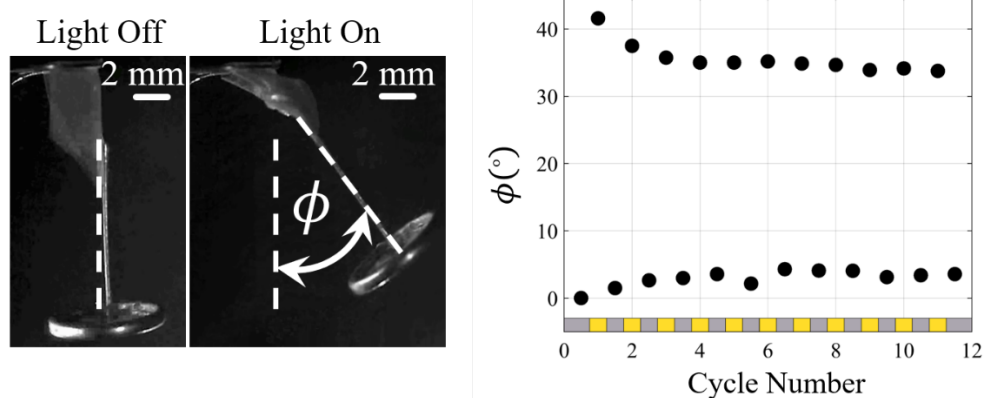


Figure SI6: Actuation over multiple on/off irradiation cycles. The angle ϕ is tracked following snap-through (x-axis yellow) as well as after it resets spontaneously in the dark (x-axis gray)

Synthesis of lower modulus azobenzene-functionalized liquid crystal polymers (ALCP-LM):

Splay ALCP-LM film were synthesized by copolymerizing a formulation composed from 19 wt% of 1,4-Bis-[4-(6-acryloyloxyhexyloxy)benzoyloxy]-2-methylbenzene (RM82), 44 wt% of 4-[[6-[(1-Oxo-2-propen-1-yl)oxy]hexyl]oxy]benzoic Acid 4-methoxyphenyl Ester, 16 wt% of 4-[[6-[(1-Oxo-2-propen-1-yl)oxy]hexyl]oxy]benzoic Acid 4-methoxyphenyl Ester, 14 wt % of 2,2' (Ethylenedioxy)diethanethiol (EDDT), 6 wt % of 4,4'-(di(6 (acryloxy)hexyloxy)azobenzene) and 1 wt% photoinitiator Irgacure (I-784) to a glass vial and thoroughly mixing. To make a splayed molecular orientation sample one glass side was coated with Elvamide (Dupont 8023R) and rubbed. The other glass slide was coated with a material that induces homeotropic alignment Nissan Chemical SE5661. The, the slides were glued together with 50 μm silica spacers. The monomer mixture was filled into the gap of the splay aligned cells by capillary action in a dark room conditions on a hotplate at 100°C. Then, the sample was cooled to the nematic phase $\sim 45^\circ\text{C}$ and polymerized using light for 60 min. An Edmund MI-150 high-intensity illuminator equipped with a cut off filter ($\lambda \geq 420\text{ nm}$, 35 mW/ cm^2) was used.

References:

1. N. P. Bende, et al., Geometrically controlled snapping transitions in shells with curved creases. Proc. Natl. Acad. Sci. U. S. A. 112, 11175–11180 (2015).

SI Movie Captions:

SI Movie 1: Actuation of $R=3.7\text{mm}$ sample that is overlaid with the simulation.

SI Movie 2: Actuation of $R=2.2\text{mm}$ sample that is overlaid with the simulation.

SI Movie 3: Harnessing the flexural actuation from snap-through in a vertical lifter.

SI Movie 4: Harnessing the flexural actuation from snap-through in a gripper.

SI Movie 5: Benchmarking the torque-dense actuation in the presence of a load.

SI Movie 6: Optically modulated photomechanical actuation.

Table SI1: Data used to populate the property-space map in Figure 2c

Type	Model	Torque (N.m)	Weight (gr)	Torque Density (N.m/K.gr)	Rotational Speed (rad/sec)
Pneumatic					
	phd-RA Series	1.6	8.20E+02	1.95E+00	62.83
	https://www.phdinc.com/product/?product=rolary-actuators&series=ra#/Catalog	1.6	8.20E+02	1.95E+00	62.83
		1.6	1.04E+03	1.54E+00	62.83
		3.1	1.09E+03	2.84E+00	62.83
		3.1	1.27E+03	2.44E+00	62.83
		3.1	1.63E+03	1.90E+00	62.83
		6.8	1.95E+03	3.49E+00	62.83
		6.8	2.22E+03	3.06E+00	62.83
		6.8	2.94E+03	2.31E+00	62.83
		12.8	3.49E+03	3.67E+00	41.89
		12.8	3.99E+03	3.21E+00	41.89
		12.8	5.35E+03	2.39E+00	41.89
		24.9	5.26E+03	4.73E+00	41.89
		24.9	5.81E+03	4.29E+00	41.89
		24.9	8.03E+03	3.10E+00	41.89
	RL Series	0.5	1.30E+02	3.85E+00	104.72
	https://www.phdinc.com/product/?product=rolary-actuators&series=rl#/Catalog	0.5	1.80E+02	2.78E+00	104.72
		0.5	1.80E+02	2.78E+00	104.72
		1	1.80E+02	5.56E+00	104.72
		1	2.20E+02	4.55E+00	104.72
		1	2.70E+02	3.70E+00	104.72
		2	3.20E+02	6.25E+00	62.83
		2	3.60E+02	5.56E+00	62.83
		2	4.10E+02	4.88E+00	62.83
		3.7	5.00E+02	7.40E+00	62.83
		3.7	5.40E+02	6.85E+00	62.83
		3.7	6.40E+02	5.78E+00	62.83
		7.7	7.70E+02	1.00E+01	62.83
		7.7	9.10E+02	8.46E+00	62.83
		7.7	1.04E+03	7.40E+00	62.83
		16	1.17E+03	1.37E+01	52.36
		16	1.49E+03	1.07E+01	52.36
		16	1.95E+03	8.21E+00	52.36
		29.9	2.36E+03	1.27E+01	41.89
		29.9	2.72E+03	1.10E+01	41.89
		29.9	3.13E+03	9.55E+00	41.89
		59.4	4.17E+03	1.42E+01	41.89
		59.4	4.76E+03	1.25E+01	41.89
		59.4	5.57E+03	1.07E+01	41.89

	RCC Series	https://www.phidinc.com/product/?product=rotary-actuators&series=rcc/Catalog	0.2037	1.50E+02	1.36E+00	19.63
			0.2037	1.40E+02	1.46E+00	19.63
			0.5656	3.00E+02	1.89E+00	13.09
			0.5656	2.80E+02	2.02E+00	13.09
			1.5491	5.50E+02	2.82E+00	13.09
			1.5491	5.30E+02	2.92E+00	13.09
	RF Series		0.748	2.80E+02	2.67E+00	8.98
		https://www.phidinc.com/product/?product=rotary&series=r/Catalog	2.72	8.50E+02	3.20E+00	7.31
			7.412	1.56E+03	4.75E+00	8.49
	RI Series		4.148	1.36E+03	3.05E+00	24.17
		https://www.phidinc.com/product/?product=rotary-actuators&series=r/Catalog	8.228	1.59E+03	5.17E+00	13.66
			4.148	1.86E+03	2.23E+00	13.66
			8.16	3.44E+03	2.37E+00	28.56
			16.184	3.63E+03	4.46E+00	11.22
			8.16	4.36E+03	1.87E+00	11.22
			26.52	6.48E+03	4.09E+00	24.17
			53.04	6.80E+03	7.80E+00	11.22
			26.52	7.98E+03	3.32E+00	11.22
A-601.025	A-60x Pigtide RT Rotary Air Bearing Module	https://www.physikinstrumente.com/en/products/air-bearing-stages/a-60x-pigtide-rt-rotary-air-bearing-module-900719/#specification	0.57	1.50E+02	3.80E+00	314.16
A-602.038			1.13	4.00E+02	2.83E+00	314.16
A-603.025			1.7	7.00E+02	2.43E+00	314.16
A-603.050			4.52	8.00E+02	5.65E+00	314.16
A-604.050			22.6	2.10E+03	1.08E+01	314.16
A-604.090			36.7	2.60E+03	1.41E+01	314.16
A-605.065			39.6	4.60E+03	8.61E+00	209.44
A-605.100			67.8	5.30E+03	1.28E+01	209.44
A-607.075			141.3	1.94E+04	7.28E+00	104.72
A-607.175			282.5	2.60E+04	1.09E+01	104.72
AC Rotary Actuator						
(Exlar)	R2M/G075 (https://exlar.com/product/trix-iac-rotary-actuator/specs/)		2.8	3.40E+03	8.24E+01	418.88
			4.75	4.20E+03	1.13E+00	314.16
			6.33	4.90E+03	1.29E+00	209.44
	R2M/G090		6.8	6.40E+03	1.06E+00	418.88
			9	6.40E+03	1.41E+00	314.16

		power-050 - AC	56.6	2.36E+04	2.40E+00	523.60
			56.6	2.51E+04	2.25E+00	523.60
			15.6	1.94E+04	8.04E-01	523.60
		power-110 - AC	88	5.88E+04	1.50E+00	439.82
			88	5.96E+04	1.48E+00	439.82
			44.2	5.23E+04	8.45E-01	471.24
DC Rotary Actuator						
(Tritek II)	RDM/G060 (https://exlar.com/product/tritek-ii-rotary-actuator/specs/)		1.44	1.40E+03	1.03E+00	523.60
			1.5	1.90E+03	7.89E-01	523.60
			1.92	2.40E+03	8.00E-01	418.88
	RDM/G075		2.08	3.40E+03	6.12E-01	418.88
			3.16	4.20E+03	7.52E-01	314.16
	RDM/G090		4.63	4.90E+03	9.45E-01	209.44
			2.46	5.70E+03	4.32E-01	345.58
			4.07	7.00E+03	5.81E-01	188.50
			5.97	8.40E+03	7.11E-01	146.61
Miniature High Torque DC Motors	C13-L19-10		0.353	1.93E+02	1.83E+00	314.16
Miniature High Torque DC Motors	C13-L19-20		0.353	1.93E+02	1.83E+00	196.87
Miniature High Torque DC Motors	C13-L19-30		0.353	1.93E+02	1.83E+00	301.07
Miniature High Torque DC Motors	C13-L19-40		0.353	1.93E+02	1.83E+00	233.00
Miniature High Torque DC Motors	C13-L19-50		0.353	1.93E+02	1.83E+00	301.28
Miniature High Torque DC Motors	C13-L25-10		0.53	2.55E+02	2.08E+00	251.33
Miniature High Torque DC Motors	C13-L28-10		0.706	3.18E+02	2.22E+00	172.05
Miniature High Torque DC Motors	C13-L28-20		0.706	3.18E+02	2.22E+00	255.41
Miniature High Torque DC Motors	21105N-03		0.053	8.31E+01	6.38E-01	680.68
DC Cube Torque Motors	21105A-04		0.053	8.31E+01	6.38E-01	680.68
DC Cube Torque Motors	21105N-08		0.061	8.31E+01	7.34E-01	680.68
DC Cube Torque Motors	21105N-10		0.042	8.31E+01	5.06E-01	680.68
DC Cube Torque Motors	21105N-12		0.046	8.31E+01	5.54E-01	733.04
DC Cube Torque Motors	21105N-13		0.046	8.31E+01	5.54E-01	733.04
DC Cube Torque Motors	21605A-14S		0.078	8.31E+01	9.39E-01	733.04
DC Cube Torque Motors	21607A-15S		0.085	8.31E+01	1.02E+00	680.68
DC Cube Torque Motors	21607J-16S		0.06	8.31E+01	7.22E-01	481.71
DC Cube Torque Motors	21607J-19S		0.085	8.31E+01	1.02E+00	712.09
DC Cube Torque Motors	21605A-20S		0.085	8.31E+01	1.02E+00	701.62
DC Cube Torque Motors	21105K-22S		0.051	8.31E+01	6.14E-01	356.05
DC Cube Torque Motors	22613J-01		0.025	5.67E+01	4.41E-01	523.60
DC Cube Torque Motors	22613M-01		0.025	5.67E+01	4.41E-01	523.60
DC Cube Torque Motors	23101L-01		0.071	1.22E+02	5.82E-01	607.37
DC Cube Torque Motors	23101L-02		0.085	1.22E+02	6.97E-01	575.96

DC Cube Torque Motors	24618R-04	0.012	3.54E+01	3.39E+01	523.60
DC Cube Torque Motors	24618N-05	0.019	3.54E+01	5.36E+01	599.52
DC Cube Torque Motors	24618N-09	0.007	3.54E+01	1.98E+01	628.32
DC Cube Torque Motors	24618V-10	0.018	3.54E+01	5.08E+01	575.96
DC Cube Torque Motors	24618V-11	0.011	3.54E+01	3.10E+01	691.15
DC Cube Torque Motors	24618V-15	0.007	3.54E+01	1.98E+01	523.60
TPM+ Servo Actuators(Rare Earth Permanent Magnetic)	dynamic 004 - DC	30	2.20E+03	1.36E+01	39.27
https://www.wittenstein.de/download/alpha-mechatronic-systems-tpm-en.pdf		32	2.20E+03	1.45E+01	29.95
		40	2.20E+03	1.82E+01	20.32
		32	2.00E+03	1.60E+01	10.26
		32	2.00E+03	1.60E+01	9.84
		32	2.00E+03	1.60E+01	6.91
	dynamic 010 - DC	57	4.80E+03	1.19E+01	39.27
		75	4.80E+03	1.56E+01	29.95
		100	4.80E+03	2.08E+01	20.32
		80	4.30E+03	1.86E+01	10.26
		80	4.30E+03	1.86E+01	9.84
		80	4.30E+03	1.86E+01	6.91
	dynamic 025 - DC	182	8.50E+03	2.14E+01	39.27
		239	8.50E+03	2.81E+01	29.95
		300	8.50E+03	3.53E+01	20.32
		250	7.10E+03	3.52E+01	10.26
		250	7.10E+03	3.52E+01	9.84
		250	7.10E+03	3.52E+01	6.91
	dynamic 050 - DC	435	1.85E+04	2.35E+01	32.67
		500	1.85E+04	2.70E+01	24.92
		650	1.85E+04	3.51E+01	16.86
		447	1.47E+04	3.04E+01	8.59
		469	1.47E+04	3.19E+01	8.17
		500	1.47E+04	3.40E+01	5.76
	high torque 010 - DC	230	7.60E+03	3.03E+01	23.04
		230	7.60E+03	3.03E+01	18.43
		230	7.60E+03	3.03E+01	13.19
		230	7.60E+03	3.03E+01	9.22
		230	8.00E+03	2.88E+01	5.76
		230	8.00E+03	2.88E+01	4.61
		230	6.50E+03	3.54E+01	3.25
		230	6.50E+03	3.54E+01	2.30
	high torque 025 - DC	530	1.48E+04	3.58E+01	23.04
		530	1.48E+04	3.58E+01	18.43
		530	1.48E+04	3.58E+01	13.19
		530	1.48E+04	3.58E+01	9.22

		480	1.00E+04	4.80E+01	7.64
		480	1.00E+04	4.80E+01	5.76
		480	1.00E+04	4.80E+01	4.61
		480	1.00E+04	4.80E+01	3.25
		480	1.00E+04	4.80E+01	2.30
	high torque 050 - DC	950	2.53E+04	3.75E+01	21.47
		950	2.53E+04	3.75E+01	17.17
		950	2.53E+04	3.75E+01	12.25
		950	2.53E+04	3.75E+01	8.59
		950	2.18E+04	4.36E+01	7.23
		950	2.18E+04	4.36E+01	5.76
		950	2.18E+04	4.36E+01	4.61
		950	2.18E+04	4.36E+01	3.25
		950	2.18E+04	4.36E+01	2.30
	high torque 110 - DC	560	7.68E+04	7.29E+00	19.79
		560	7.68E+04	7.29E+00	15.81
		560	7.68E+04	7.29E+00	11.31
		560	7.68E+04	7.29E+00	7.85
		560	6.38E+04	8.78E+00	6.60
		560	6.38E+04	8.78E+00	4.92
		560	4.55E+04	1.23E+01	4.29
		560	4.55E+04	1.23E+01	3.04
		560	4.55E+04	1.23E+01	2.09
	power 004 1-stage - DC	15	3.60E+03	4.17E+00	157.08
		18	3.60E+03	5.00E+00	125.66
		26	3.60E+03	7.22E+00	89.74
		26	3.60E+03	7.22E+00	62.83
	power 004 2-stage - DC	50	3.70E+03	1.35E+01	39.27
		50	3.70E+03	1.35E+01	31.42
		50	3.70E+03	1.35E+01	25.13
		50	3.70E+03	1.35E+01	22.41
		50	3.70E+03	1.35E+01	17.91
		50	3.30E+03	1.52E+01	15.71
		50	3.30E+03	1.52E+01	2.09
		50	3.30E+03	1.52E+01	9.01
		35	3.30E+03	1.06E+01	6.28
	power 010 1-stage - DC	44	7.20E+03	6.11E+00	157.08
		56	7.20E+03	7.78E+00	125.66
		80	7.20E+03	1.11E+01	89.74
		85	7.20E+03	1.18E+01	62.83
	power 010 2-stage - DC	130	7.40E+03	1.76E+01	39.27
		130	7.40E+03	1.76E+01	31.42
		130	7.40E+03	1.76E+01	25.13
		130	7.40E+03	1.76E+01	22.41
		130	7.40E+03	1.76E+01	17.91

			130	6.00E+03	2.17E+01	15.71
			130	6.00E+03	2.17E+01	12.57
			130	6.00E+03	2.17E+01	9.01
			100	6.00E+03	1.67E+01	6.28
		power 025 1 -stage - DC	112	1.40E+04	8.00E+00	157.08
			141	1.40E+04	1.01E+01	125.66
			199	1.40E+04	1.42E+01	89.74
			200	1.40E+04	1.43E+01	62.83
		power 025 2 -stage - DC	350	1.45E+04	2.41E+01	39.27
			350	1.45E+04	2.41E+01	31.42
			380	1.45E+04	2.62E+01	25.13
			350	1.45E+04	2.41E+01	22.41
			380	1.45E+04	2.62E+01	17.91
			305	1.03E+04	2.96E+01	15.71
			380	1.03E+04	3.69E+01	12.57
			330	1.03E+04	3.20E+01	9.01
			265	1.03E+04	2.57E+01	6.28
		power 110 2 -stage - DC	1375	5.96E+04	2.31E+01	29.43
			1600	5.96E+04	2.68E+01	23.56
			1600	5.96E+04	2.68E+01	18.85
			1600	5.96E+04	2.68E+01	16.86
			1600	5.96E+04	2.68E+01	13.51
			1600	5.23E+04	3.06E+01	1.26
			1600	5.23E+04	3.06E+01	9.42
			1600	5.23E+04	3.06E+01	6.70
			1400	5.23E+04	2.68E+01	4.71
		power 110 1 -stage - DC	340	5.88E+04	5.78E+00	109.96
			428	5.88E+04	7.28E+00	87.96
			603	5.88E+04	1.03E+01	67.33
			555	5.88E+04	9.44E+00	47.12
		https://www.physikinstrumente.com/en/products/rotation-stages/v-611-compact-primae-rotation-stage-412418470/#specification	1.9	1.20E+03	1.58E+00	0.84
		https://www.physikinstrumente.com/en/products/rotation-stages/v-610-compact-primae-rotation-stage-412418469/#specification	1.2	6.30E+02	1.90E+00	9.42
		https://www.physikinstrumente.com/en/products/rotation-stages/l-611-precision-rotation-stage-1202002/#specification	40	1.10E+03	3.64E+01	3.49
TPM+ Servo Actuators (Rare Earth Permanent Magnetic)	dynamic 004 - AC		2	2.20E+03	9.09E+01	628.32

https://www.wittenstein.de/download/operating-manual-tpm-plus-en.pdf							
	dynamic 010 - AC	0.98	2.00E+03	4.90E+01	628.32		
		3.8	4.80E+03	7.92E+01	628.32		
		1.9	4.30E+03	4.42E+01	628.32		
	dynamic 025 - AC	12.1	8.50E+03	1.42E+00	628.32		
		4.4	7.10E+03	6.20E+01	628.32		
	dynamic 050 - AC	28.9	1.85E+04	1.56E+00	523.60		
		7.8	1.47E+04	5.31E+01	523.60		
	dynamic 110 - AC	43.9	3.71E+04	1.18E+00	387.46		
		28.9	3.59E+04	8.05E+01	523.60		
	high torque 010 - AC	11.98	7.60E+03	1.58E+00	507.89		
		11.98	8.00E+03	1.50E+00	507.89		
		11.98	8.00E+03	1.50E+00	507.89		
		4.4	6.50E+03	6.77E+01	507.89		
	high torque 025 - AC	28.9	1.48E+04	1.95E+00	507.89		
		11.98	1.00E+04	1.20E+00	507.89		
		11.98	1.00E+04	1.20E+00	507.89		
		11.98	1.00E+04	1.20E+00	507.89		
		11.98	1.00E+04	1.20E+00	507.89		
	high torque 050 - AC	56.6	2.53E+04	2.24E+00	471.24		
		28.9	2.18E+04	1.33E+00	507.89		
		28.9	2.18E+04	1.33E+00	507.89		
		28.9	2.18E+04	1.33E+00	507.89		
		28.9	2.18E+04	1.33E+00	507.89		
		28.9	2.18E+04	1.33E+00	507.89		
		28.9	2.18E+04	1.33E+00	507.89		
	high torque 110 - AC	164.5	7.68E+04	2.14E+00	434.59		
		88	6.38E+04	1.38E+00	434.59		
		88	6.38E+04	1.38E+00	434.59		
		56.6	4.55E+04	1.24E+00	471.24		
		56.6	4.55E+04	1.24E+00	471.24		
		3.8	3.60E+03	1.06E+00	628.32		
	power 004 - AC	3.8	3.70E+03	1.03E+00	628.32		
		1.9	3.30E+03	5.76E+01	628.32		
		12.1	7.20E+03	1.68E+00	628.32		
	power 010 - AC	12.1	7.40E+03	1.64E+00	628.32		
		4.4	6.00E+03	7.33E+01	628.32		
		28.9	1.40E+04	2.06E+00	628.32		
	power 025 - AC	28.9	1.45E+04	1.99E+00	628.32		
		7.8	1.03E+04	7.57E+01	628.32		
	power 050 - AC	56.6	2.36E+04	2.40E+00	523.60		
		56.6	2.51E+04	2.25E+00	523.60		
		15.6	1.94E+04	8.04E+01	523.60		
	power 110 - AC	88	5.88E+04	1.50E+00	439.82		
		88	5.96E+04	1.48E+00	439.82		
		44.2	5.23E+04	8.45E+01	471.24		

Hydraulic

	HKS DZK and DEK Series(track and pinion)						
		1600	2.50E+04	6.40E+01	5.71		
		3200	4.50E+04	7.11E+01	5.71		
		6300	7.50E+04	8.40E+01	4.19		
		12600	1.10E+05	1.15E+02	2.51		
		25600	2.20E+05	1.16E+02	1.80		
		49500	5.00E+05	9.90E+01	1.26		
		69800	5.80E+05	1.20E+02	1.26		
		101000	8.50E+05	1.19E+02	0.79		
		141500	1.10E+06	1.29E+02	0.63		
		190000	1.50E+06	1.27E+02	0.52		
		490	1.80E+04	2.72E+01	7.85		
		910	2.50E+04	3.64E+01	7.85		
		1790	4.00E+04	4.48E+01	5.24		
		3250	1.10E+05	2.95E+01	5.24		
		5650	1.00E+05	5.65E+01	2.86		
		10600	1.60E+05	6.63E+01	2.51		
		15110	2.20E+05	7.05E+01	1.80		
		21710	3.00E+05	7.24E+01	1.80		
		29310	4.20E+05	6.98E+01	1.40		
		40710	5.50E+05	7.40E+01	1.40		
		93	5.00E+03	18.600	90.478		
EATON Xcel Motors	XLH Series (016-53)	116	5.30E+03	21.887	84.404		
EATON Xcel Motors	XLH Series (016-63)	145	5.50E+03	26.364	88.802		
EATON Xcel Motors	XLH Series (016-80)	181	6.10E+03	29.672	71.000		
EATON Xcel Motors	XLH Series (016-100)	223	6.20E+03	35.968	57.701		
EATON Xcel Motors	XLH Series (016-125)	260	6.40E+03	40.625	44.087		
EATON Xcel Motors	XLH Series (016-160)	324	6.70E+03	48.358	35.709		
EATON Xcel Motors	XLH Series (016-200)	391	7.10E+03	55.070	29.531		
EATON Xcel Motors	XLH Series (016-245)	508	7.40E+03	68.649	21.886		
EATON Xcel Motors	XLH Series (016-315)	547	7.70E+03	71.039	17.907		
EATON Xcel Motors	XLH Series (016-390)	507	8.00E+03	63.375	14.451		
EATON Xcel Motors	XLH Series (016-485)	116	6.30E+03	18.413	91.630		
EATON Xcel Motors	XLH Series (036-50)	192	7.00E+03	27.429	86.917		
EATON Xcel Motors	XLH Series (036-80)	241	7.50E+03	32.133	69.639		
EATON Xcel Motors	XLH Series (036-100)	273	7.70E+03	35.455	53.931		
EATON Xcel Motors	XLH Series (036-130)	328	7.10E+03	46.197	44.506		
EATON Xcel Motors	XLH Series (036-160)	379	8.00E+03	47.375	36.024		
EATON Xcel Motors	XLH Series (036-195)	437	8.40E+03	52.024	28.798		
EATON Xcel Motors	XLH Series (036-245)	444	9.40E+03	47.234	22.515		
EATON Xcel Motors	XLH Series (036-305)	512	9.60E+03	53.333	17.907		
EATON Xcel Motors	XLH Series (036-395)	345	7.30E+03	47.260	95.086		

EATON Xcel Motors	XI2 Series (100)	445	7.50E+03	59.333	96.761
EATON Xcel Motors	XI2 Series (130)	560	7.70E+03	72.727	75.294
EATON Xcel Motors	XI2 Series (160)	570	7.90E+03	72.152	74.665
EATON Xcel Motors	XI2 Series (195)	665	8.40E+03	79.167	60.423
EATON Xcel Motors	XI2 Series (245)	820	8.80E+03	93.182	48.381
EATON Xcel Motors	XI2 Series (305)	885	9.30E+03	95.161	38.223
EATON Xcel Motors	XI2 Series (395)	925	9.80E+03	94.388	30.055
EATON Xcel Motors	XI2 Series (490)	930	1.02E+04	91.176	24.086
EATON Xcel Motors	XI4 Series (160)	705	1.41E+04	50.000	72.571
EATON Xcel Motors	XI4 Series (205)	800	1.45E+04	55.172	57.177
EATON Xcel Motors	XI4 Series (245)	845	1.47E+04	57.483	55.711
EATON Xcel Motors	XI4 Series (310)	1065	1.56E+04	68.269	44.192
EATON Xcel Motors	XI4 Series (395)	1185	1.66E+04	71.386	39.375
Hydraulic	XI4 Series (495)	1170	1.79E+04	65.363	31.940
Piezo					
	Rotary Piezo Actuator(http://www.cedrat-technologies.com/en/technologies/actuators/piezo-motors-and-electronics.html)	0.15	330	4.55E-01	14.66
	Q-622 Q-Motion® Miniature Rotation Stage (https://www.physikinstrumente.com/en/products/miniature-stages/miniature-rotation-stages/q-622-q-motion-miniature-rotation-stage-103190/)	5.00E-03	15	3.33E-01	1.22
		5.00E-03	12	4.17E-01	1.22
		5.00E-03	12	4.17E-01	1.22
		6.00E-03	25	2.40E-01	0.79
		6.00E-03	21	2.86E-01	0.79
		6.00E-03	21	2.86E-01	0.79
		5.00E-03	9	5.56E-01	1.22
		5.00E-03	9	5.56E-01	1.22
		0.3	500	6.00E-01	9.42
	https://www.physikinstrumente.com/en/products/miniature-stages/miniature-rotation-stages/n-651-rotation-stage-with-low-profile-design-703071/#specification	0.03	300	1.00E-01	12.57
	https://www.physikinstrumente.com/en/products/miniature-stages/miniature-rotation-stages/n-622-pilze-rotation-stage-703081/#specification	0.005	120	4.17E-02	12.57

	https://www.physikinstrumente.com/en/products/miniature-stages/miniature-rotation-stages/l-624-pilne-rotation-stage-7030690/#specification	0.01	130	7.69E-02	12.57
	https://www.cedrat-technologies.com/fileadmin/user_upload/CTH/C/Technologies/Actuators/Piezo_motors_electronics/fiche_RPA/Rotary_Piezo_Motor_RPA.pdf	0.15	330	4.55E-01	14.66
	https://www.physikinstrumente.com/en/products/miniature-stages/miniature-rotation-stages/l-628-pilne-rotation-stage-7030660/#specification	0.025	300	8.33E-02	12.57
	https://www.physikinstrumente.com/en/products/miniature-stages/miniature-rotation-stages/q-632-g-motion-rotation-stage-111229/#specification	0.007	25	2.80E-01	0.35
Piezo LEGS	LR17 version A21 - Standard - With Position Sensor	0.015	30	5.00E-01	2.97
Piezo LEGS	LR50 version 12D - Non-Magnetic - Vacuum	0.025	60	4.17E-01	1.75
Piezo LEGS	LR80 version 12A - Standard	0.04	60	6.67E-01	1.75
Piezo LEGS	LR80 version 12B - Vacuum	0.04	60	6.67E-01	1.75
SMA					
	https://iopscience.iop.org/article/10.1088/0964-1726/21/6/065013/meta	4.20E-03	0.05	8.40E+01	1.75
	https://iopscience.iop.org/article/10.1088/0964-1726/19/12/125014	4.70E-03	3.30E-02	1.42E+02	1.01
		4.50E-03	0.035	1.29E+02	0.92
		4.50E-03	3.50E-02	1.29E+02	1.26
	https://www.sciencedirect.com/science/article/pii/S0924424719300573	0.0733	10.2	7.19E+00	1.87
	https://www.sciencedirect.com/science/article/pii/S0924424709005169#fig2	1.96	0.8	2.45E+03	4.19

Weight is an estimation of SMA material only_ Torque is 0.14*30d_ Velocity is for 30d and 2A current